Lecture 6

p+p, Helium Burning and Energy Generation

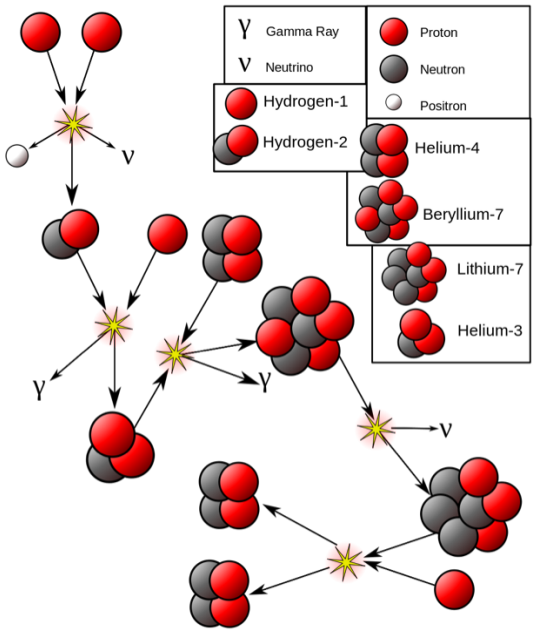

Proton-proton reaction:

$$p(p,e^+\nu_e)^2\mathrm{H} \quad (+0.42\,\mathrm{MeV})$$

see Lecture 4 for energy yield

This cross section is far too small (~10^{-47} cm^2 at 1 MeV) to measure in the laboratory, but it does have a nearly constant, calculable S-factor.

The theory is straightforward, but complex (e.g., Clayton 366 - 368) because it includes a strong interaction and weak interaction happening in rapid succession.

Two stages:

- Temporarily form diproton (initial wave function can be probed experimentally with proton scattering). Initial diproton must have J = 0 because can't have protons in identical states.
- Diproton experiences a weak interaction (with a spin flip) to make deuteron ^{2}H(J^π.=1^+)

We shall be terse in our discussion of this reaction, chiefly because it involves a lot of concepts we have not discussed so far (weak decays, axial/vector currents, etc), but also because it is unimportant in massive stars. Read Adelberger et al, 1998, RMP (Sec III) for background. This is given at the class website. See also Kamionkowski and Bahcall (1994)

$$S(0)=6\pi^2 m_p c\alpha \ln 2 \frac{\Lambda^2}{\gamma^3}\left(\frac{G_A}{G_V}\right)^2 \frac{f_{pp}^R}{(ft)_{0^+\to 0^+}}(1+\delta)^2$$

where α is the fine structure constant, m_p is the mass of the proton, c is the speed of light, G_V and G_A are the Fermi and axial vector weak-coupling constants, $\gamma=(2\mu E_D)=$ 0.23161 fm^{-1} is the deuteron binding wave number, μ is the proton-neutron reduced mass and E_D is the deuteron binding energy, ($\hbar$=1), f_{pp}^R is the phase space factor, $(ft)_{0^+\to 0^+}$ is the (ft) value for the superallowed $0^+\to 0^+$ transitions, Λ is proportional to the overlap of the *pp* and deuteron wave functions, and δ is a small correction to the nuclear force for the exchange of heavier mesons.

Λ^2 is given by the overlap integral between the initial *pp* wave function and the final state deuteron wave function. The wave functions are determined by integrating Schroedinger's equation for the two nucleon system with an assumed nuclear potential. The potential for the *pp* wave function must fit the data on proton-proton scattering. Five different potentials* were explored by Kamionkowski and Bahcall (1994) and give results consistent with the quoted error bar. The deuteron wave function must be consistent with the deuteron binding energy and other experimental constraints. Seven different possibilities were explored. The overall error is in Λ^2 is about 0.2%.

*square well, Gaussian, exponential Yukawa, and repulsive core

(ft) and G_A/G_V are determined by measurements of weak decay in a variety of nuclei and especially the lifetime of the free neutron. The standard value for the latter is 881 +- 2 seconds. But see Bumm, Science, **360,** 605 (2018) 888 or 879? The weak decay here is of the Gamow-Teller type ($\Delta J = 0,1$), not Fermi ($\Delta J = 0$). GT is mediated by the axial current (A). Fermi is mediated by the vector current (V).

The other factors are either accurately measurable (deuteron BE), straightforward to calculate (f_{pp}), or complicated and not very important (δ).

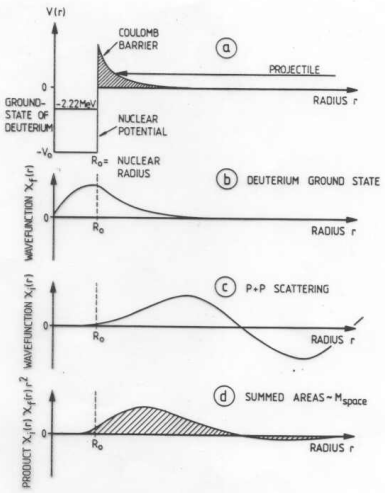

FIGURE 6.4. Shown schematically are a few ingredients used in the numerical evaluation of the space matrix element M_{space} for the $p + p \rightarrow d + e^+ + \nu$ reaction. The potential is shown in (*a*), where, for a given nuclear radius R_0, the observed binding energy of the deuterium determines the potential depth V_0. The deuterium radial wave function $\chi_f(r)$ is determined by the potential $V(r)$. Because of the loosely bound ground state, $\chi_f(r)$ extends far outside R_0 with appreciable amplitudes (*b*). The initial wave function $\chi_i(r)$ is obtained from $p + p$ elastic scattering data, which gives (*c*) a small amplitude for $r \lesssim R_0$ and has the usual oscillating pattern of a plane wave for $r \gg R_0$. The radial integrand in M_{space} (*d*) then has its major contributions in regions far outside R_0 (*hatched areas*).

Putting in best values Adelberger (1998, 2011) Rev. Mod. Phys.

$$S(0) = 4.01\times10^{-25}\ \text{MeV barns}\left(\frac{(ft)_{0^+\rightarrow0^+}}{3071.4\ \text{sec}}\right)^{-1}\left(\frac{\Lambda^2}{7.035}\right)$$

$3.78 \pm 0.15 \times 10^{-25}$ in Bahcall (1968)

$$\times\left(\frac{G_A/G_V}{1.2695}\right)^2\left(\frac{f_{pp}^R}{0.144}\right)\left(\frac{1+\delta}{1.01}\right)^2$$

theoretical

$$S(0) = 4.01\pm0.04\times10^{-25}\ \text{MeV barns}$$

The overlap is insensitive to the form of nuclear potential assumed inside a few fm and is determined by the tail of the potential at the nuclear surface.

This is highly constrained by proton scattering experiments.

History:

Bethe and Critchfield (1938)
Salpeter (1952)

Adelberger et al (2011), *Rev. Mod. Phys.* **83**, 195

TABLE I The Solar Fusion II recommended values for S(0), its derivatives, and related quantities, and for the resulting uncertainties on S(E) in the region of the solar Gamow peak – the most probable reaction energy – defined for a temperature of 1.55×10^7K characteristic of the Sun's center. See the text for detailed discussions of the range of validity for each S(E). Also see Sec. VIII for recommended values of CNO electron capture rates, Sec. XI.B for other CNO S-factors, and Sec. X for the ^{8}B neutrino spectral shape. Quoted uncertainties are 1σ.

Reaction	Section	S(0) (keV-b)	S′(0) (b)	S″(0) (b/keV)	Gamow peak uncertainty (%)
$p(p,e^+\nu_e)d$	III	$(4.01 \pm 0.04)\times10^{-22}$	$(4.49 \pm 0.05)\times10^{-24}$	–	± 0.7
$d(p,\gamma)^3He$	IV	$(2.14^{+0.17}_{-0.16})\times10^{-4}$	$(5.56^{+0.18}_{-0.20})\times10^{-6}$	$(9.3^{+3.9}_{-3.4})\times10^{-9}$	± 7.1 [a]
$^3He(^3He,2p)^4He$	V	$(5.21 \pm 0.27) \times 10^3$	-4.9 ± 3.2	$(2.2 \pm 1.7) \times 10^{-2}$	± 4.3 [a]
$^3He(^4He,\gamma)^7Be$	VI	0.56 ± 0.03	$(-3.6 \pm 0.2)\times10^{-4}$ [b]	$(0.151 \pm 0.008)\times10^{-6}$ [c]	± 5.1
$^3He(p,e^+\nu_e)^4He$	VII	$(8.6 \pm 2.6)\times10^{-20}$	–	–	± 30
$^7Be(e^-,\nu_e)^7Li$	VIII	See Eq. (40)	–	–	± 2.0
$p(pe^-,\nu_e)d$	VIII	See Eq. (46)	–	–	± 1.0 [d]
$^7Be(p,\gamma)^8B$	IX	$(2.08 \pm 0.16)\times10^{-2}$ [e]	$(-3.1 \pm 0.3)\times10^{-5}$	$(2.3 \pm 0.8)\times10^{-7}$	± 7.5
$^{14}N(p,\gamma)^{15}O$	XI.A	1.66 ± 0.12	$(-3.3 \pm 0.2)\times10^{-3}$ [b]	$(4.4 \pm 0.3)\times10^{-5}$ [c]	± 7.2

[a] Error from phenomenological quadratic fit. See text.
[b] S′(0)/S(0) taken from theory; error is that due to S(0). See text.
[c] S″(0)/S(0) taken from theory; error is that due to S(0). See text.
[d] Estimated error in the pep/pp rate ratio. See Eq. (46)
[e] Error dominated by theory.

Helium Burning

Helium burning is a two-stage nuclear process in which two alpha-particles temporarily form the ground state of unstable ^{8}Be*. Occasionally the ^{8}Be* captures a third alpha-particle before it flies apart. No weak interactions are involved.

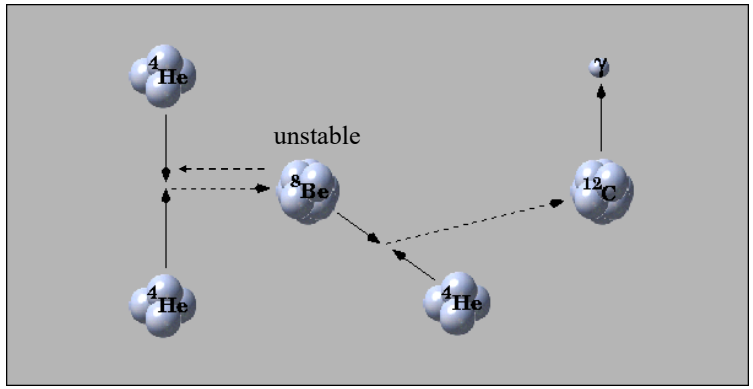

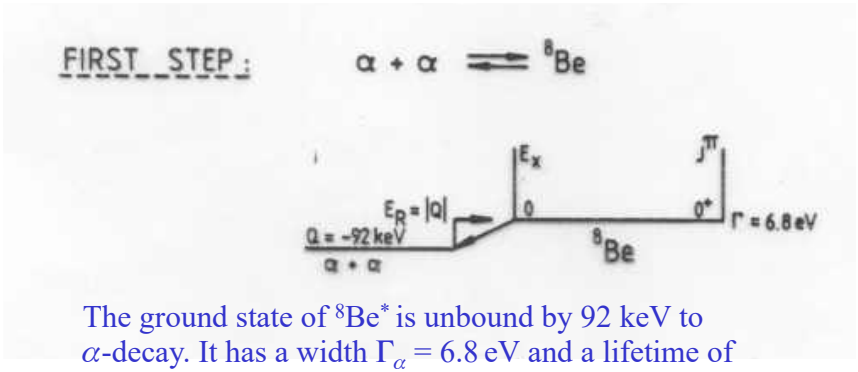

The ground state of ^{8}Be* is unbound by 92 keV to α-decay. It has a width $\Gamma_\alpha = 6.8$ eV and a lifetime of

$$\tau = \frac{\hbar}{\Gamma} = \frac{6.58 x 10^{-22}\ \text{MeV s}}{6.8 x 10^{-6}\ \text{MeV}} = 9.7 x 10^{-17}\ \text{sec}$$

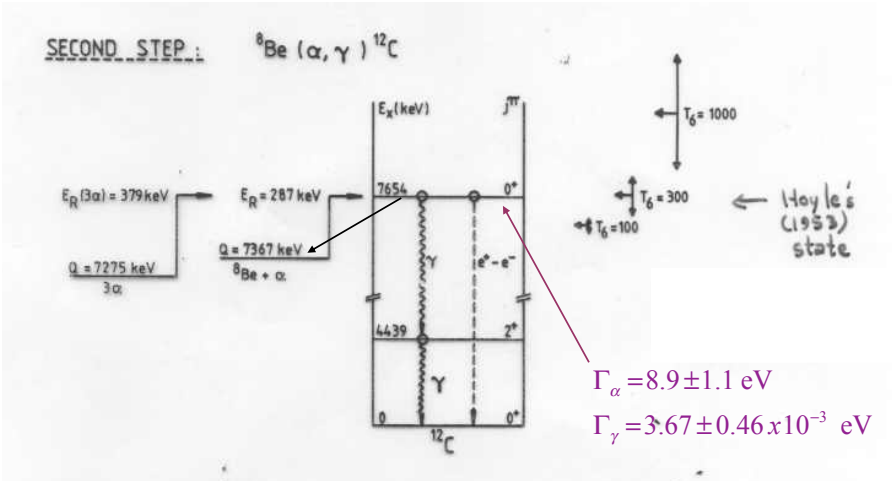

The 7.654 MeV excited state of ^{12}C plays a critical role in the 3α reaction. Its α-width is much greater than its photon width, so it predominantly decays back to ^{8}Be*, setting up an equilibrium abundance of ^{12}C*. Γ_γ is augmented by a small contribution from pair production.

Recall the Saha equation: (e.g., Clayton p 29). For example, for ionized and neutral hydrogen:

$$\frac{n(\text{H II})\, n_e}{n(\text{H I})} = \frac{G(\text{H II})\ g_e}{G(\text{H I})}\left[\frac{(2\pi m_e kT)^{3/2}}{h^3}\right]\exp(-\chi_r / kT)$$

The same thermodynamic arguments (equilibrium, chemical potential, etc.)also give a *nuclear* Saha equation. In particular, the equilibrium concentration of an unbound transitory ^{8}Be* nucleus is given by

$^8Be^* \rightleftharpoons 2\ ^4He$

$$\frac{n_\alpha^2}{n(^8\text{Be})} = \left(\frac{G_\alpha^2}{G(^8\text{Be}^*)}\right)\left(\frac{(2\pi \hat{A} kT)^{3/2}}{N_A^{3/2} h^3}\right)\exp\left(\frac{-Q_{\alpha\gamma}(^4\text{He})}{kT}\right)$$

$G(^8\text{Be}^*) = 1$ (G = 2J+1)

$5.94\times10^{33}\ \hat{A}^{3/2}\ T_9^{3/2}$

$Q_{\alpha\gamma}(^4\text{He}) = \text{BE}(^8\text{Be}^*) - 2\,\text{BE}(\alpha) = 56.4995 - 2(28.2957)$

$= -0.0919$ MeV $\qquad Q_{\alpha\gamma}(^4\text{He})/kT = -0.0919 \times 11.6045/T_9 = -1.066/T_9$

$$n(^8\text{Be}^*) = \left(5.94\times10^{33}\, 2^{3/2}\, T_9^{3/2}\right)^{-1} n_\alpha^2 \exp(-1.066/T_9)$$

$$n(^8\text{Be}^*) = n_\alpha^2\, T_9^{-3/2}\,(5.95\times10^{-35})\exp(-1.066/T_9)\ \text{cm}^{-3}$$

$$\hat{A} = \frac{4\times4}{4+4} = 2$$

or, since $n \equiv \rho N_A Y$ and $Y = \frac{X}{A}$

$$X(^8\text{Be}^*) = 1.79\times10^{-11}\ \frac{\rho X_\alpha^2}{T_9^{3/2}}\ e^{-1.066/T_9}$$

For example, at 2×10^8 K, $\rho = 10^3\ \text{g cm}^{-3}, X_\alpha = 1$

$X(^8\text{Be}^*) \approx 10^{-9}$ $\qquad$ n =7.3 x 10^{16} /cm^3

This works because the dominant decay mode of ^{8}Be* is to the same products from which it is assembled, i.e.,

$$\alpha + \alpha \rightleftarrows {}^8\text{Be}^*$$

The time scale for establishing this equilibrium is very short.

Now consider the excited state of ^{12}C at 7.6542 MeV. Call it ^{12}C*. It also has as its dominant width, $\Gamma_\alpha >> \Gamma_\gamma$. That is $^8\text{Be}^* + \alpha \rightleftarrows {}^{12}\text{C}^*$

$$\frac{n(^8Be^*)n_\alpha}{n(^{12}C^*)} = 5.94\times10^{33} T_9^{3/2}\left(\frac{4\cdot8}{4+8}\right)^{3/2} e^{-Q_{\alpha\gamma}(^8Be^*)/kT}$$

$$n(^{12}\text{C}^*) = (5.94\times10^{33})^{-1}\, T_9^{-3/2}\left(\frac{12}{32}\right)^{3/2} n(^8Be^*)n_\alpha \exp(-0.287/kT)$$

where $Q_{\alpha\gamma}(^8Be^*) = BE(^{12}C) - BE(^8Be^*) - BE(\alpha) - 7.6542$

$= 92.1617 - 56.4995 - 28.2957 - 7.6542$ MeV

$= -0.2870$ MeV $\quad (*1/k = 11.6045 \Rightarrow -3.330)$

$$n(^{12}\text{C}^*) = 3.87\times10^{-35}\, T_9^{-3/2}\, n(^8Be^*)n_\alpha \exp(-3.330/T_9)$$

$$= 3.87\times10^{-35}(5.95\times10^{-35})T_9^{-3} n_\alpha^3 \exp(-3.330/T_9 - 1.066/T_9)$$

$$= 2.303\times10^{-69}\, T_9^{-3} n_\alpha^3 \exp(-4.396/T_9)$$

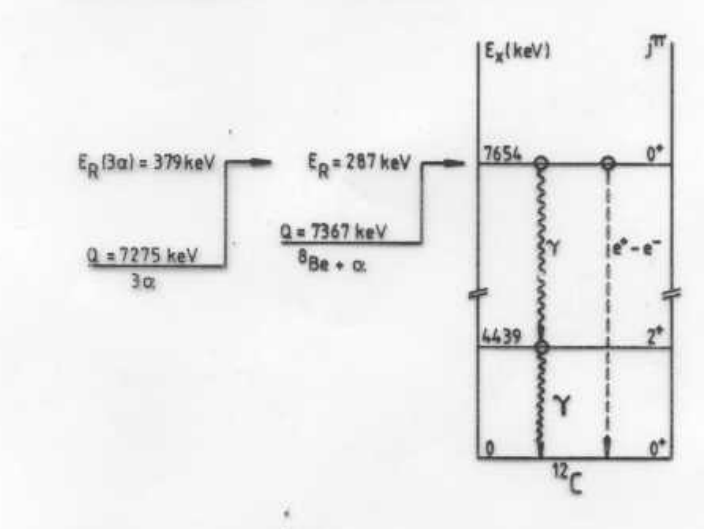

The number of ^{12}C formed permanently per second is

$$R_{3\alpha} = n(^{12}C^{*})\,\frac{\Gamma_{rad}}{\hbar}$$

Γ_{rad} is the one thing besides binding energies and excited state energy that has to be measured

$$\Gamma_{rad} = 3.41 \pm 1.12 \times 10^{-3}\ \text{eV}\ \ (1976)$$
$$= 3.67 \pm 0.46\ \text{meV}\ (1988)$$
$$= 3.64 \pm 0.5\ \text{meV}\ (1990)$$

$$\Gamma_{e^{\pm}} = 60.5 \pm 3.9\ \mu\text{eV}$$

see article by Hale (1997). Current error about 10% (Sam Austin 2013)

The current value is due to Caughlan and Fowler (1988) using mesurements from Sam Austin

$$\lambda_{3\alpha} = 2.79 \times 10^{-8}\ T_9^{-3}\ \exp(-4.396 / T_9)$$

Slight revisions to Γ_γ here

T_9	$\frac{d \ln \lambda}{d \ln T}$	
0.1	41	$= \frac{4.396}{T_9} - 3$
0.2	19	
0.3	12	

Unlike most reactions in astrophysics, the temperature dependence here is not determined by barrier penetration but by the Saha equation. In fact, at high temperature ($T_9 > 1.5$) the rate saturates and actually begins to decline slowly as the resonance slips out of the Gamow window.

This gives:

$$R_{3\alpha} = 1.28 \times 10^{-56}\ T_9^{-3}\ n_\alpha^3 \exp(-4.396 / T_9)\ \text{cm}^{-3}\ \text{sec}^{-1}$$

$$\frac{dn_{12}}{dt} = R_{3\alpha} \qquad \frac{dn_\alpha}{dt} = -3R_{3\alpha}$$

converting to our standard, Y_i notation

$$n_\alpha = \rho N_A Y_\alpha \qquad Y_\alpha = \frac{X(^4\text{He})}{4}$$

$$n_{12} = \rho N_A Y_{12} \qquad Y_{12} = \frac{X(^{12}\text{C})}{12}$$

$$\frac{dY_{12}}{dt} = \rho^2 Y_\alpha^3 (\lambda_{3\alpha} / 3!) \qquad \frac{dY_\alpha}{dt} = -3\rho^2 Y_\alpha^3 (\lambda_{3\alpha} / 3!)$$

where

$$\lambda_{3\alpha} = 3! \times N_A^2\ R_{3\alpha} = 2.79 \times 10^{-8}\ T_9^{-3} \exp(-4.396 / T_9)\ \text{cm}^6\ \text{gm}^{-2}\ \text{Mole}^{-2}\ \text{sec}^{-1}$$

(the units are such that $\rho^2 Y_\alpha^3 \lambda_{3\alpha}$ has units of Mole/s)

Helium burning 2 – the $^{12}C(\alpha,\gamma)$ rate

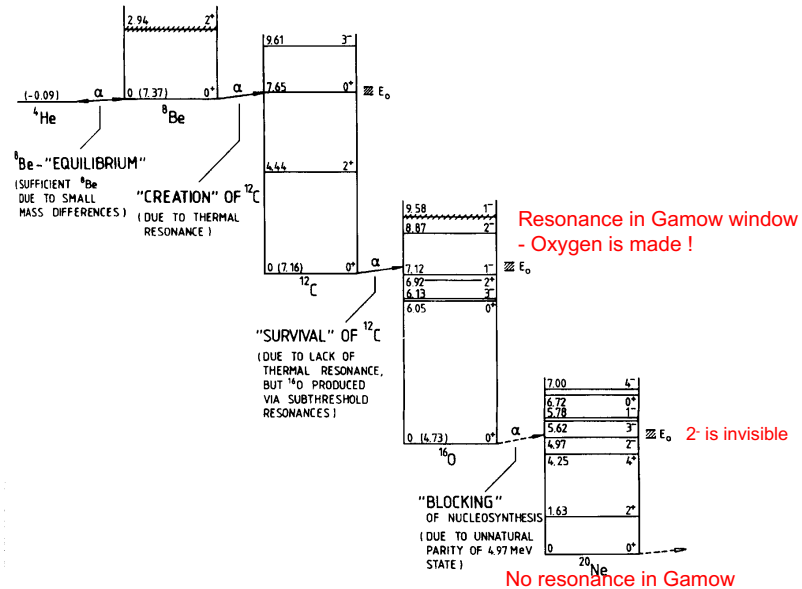

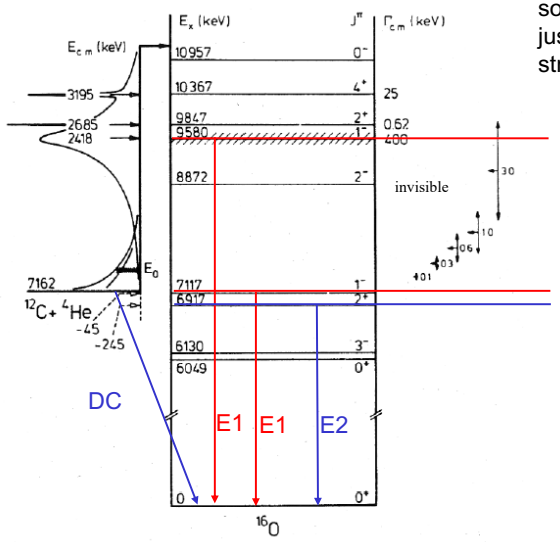

some tails of resonances just make the reaction strong enough …

resonance (high lying)

resonance (sub threshold)

resonance (sub threshold)

complications:

- very low cross section makes direct measurement impossible
- subthreshold resonances cannot be measured at resonance energy
- Interference between the E1 and the E2 components

Sub-threshold resonances

(See Rolfs and Rodney, *Cauldrons in the Cosmos*, p. 185ff)

$$\sigma(E)=\pi\lambda\!\!\!^{-2}\omega\,\frac{\Gamma_1(E)\,\Gamma_2(E+Q)}{\left(E-E_r\right)^2+\left[\Gamma(E)/2\right]^2}$$

E.g, 1 is an α-particle and 2 is a photon. Γ_1 is the probability that the α penetrates to the nuclear surface. Γ_2 is the photon width evaluated at E + Q. e.g., for dipole radiation

$$\Gamma_2=\left(\frac{E+Q}{\varepsilon_r}\right)^3\Gamma_\gamma(\varepsilon_r)$$

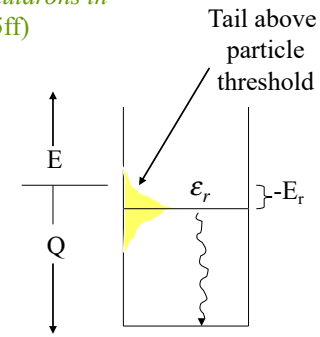

An excited state of a compound nucleus lies E_r below the threshold of the reaction, Q. The excited state is known to decay by γ emission and is characterized by a width Γ_γ. Because of this width the state extends energetically to both sides of E_r on a rapidly decreasing scale.

Uncertainty in the $^{12}C(\alpha,\gamma)$ rate was, for an extended time, the single most important nuclear physics uncertainty in astrophysics

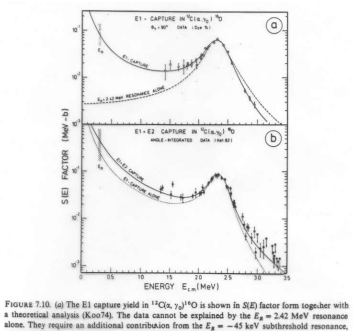

FIGURE 7.10. (a) The E1 capture yield in $^{12}C(\alpha,\gamma_0)^{16}O$ is shown in $S(E)$ factor form together with a theoretical analysis (Koo74). The data cannot be explained by the $E_x = 2.42$ MeV resonance alone. They require an additional contribution from the $E_x = -45$ keV subthreshold resonance.

Affects:

- C/O ratio → further stellar evolution (C-burning or O-burning ?)
- iron (and other) core sizes (outcome of SN explosion)

TABLE I Astrophysical environments and burning stages where the $^{12}C(\alpha,\gamma)^{16}O$ reaction plays an important role. The temperatures of these environments dictate the energy ranges where the $^{12}C(\alpha,\gamma)^{16}O$ cross section must well known for an accurate calculation of the reaction rate.

Burning Stages	Astro. Sites	Temp. Range (GK)	Gamow Energy Range (MeV)
Core Helium Burning	AGB stars and Massive Stars	0.1-0.4	0.15-0.65
Core Carbon and Oxygen Burning	Massive Stars	0.6-2.7	0.44-2.5
Core Silicon Burning	Massive Stars	2.8-4.1	1.1-3.4
Explosive Helium Burning	Supernovae and X-Ray Bursts	≈1	0.6-1.25
Explosive Oxygen and Silicon Burning	Supernovae	>5	>1.45

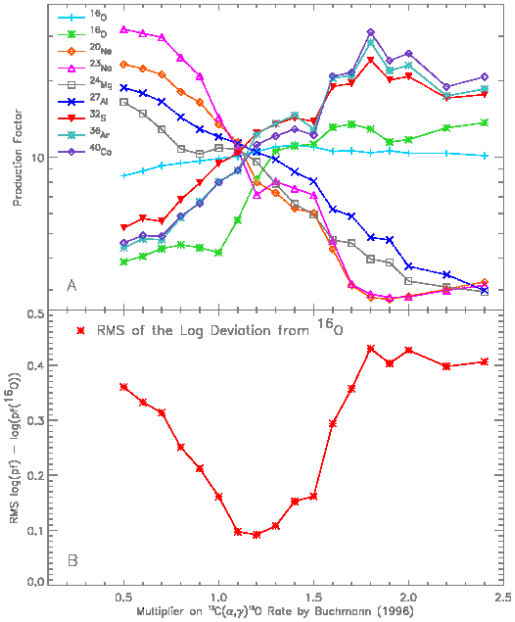

Woosley and Weaver, Physics Reports (2007)

Prediction:
S(300 keV) = 170 keV-barns

See also Woosley & Weaver, *Phys. Reports*, **227**, 65, (1993)

Buchmann, L. 1996, ApJ, 468, L127 gives fits good at both low and hi T

Kunz et al., ApJ, 567, 643, (2002)

$S_{E1}(300\ \text{keV}) = 76 +/- 20\ \text{keV b}$

$S_{E2}(300\ \text{keV}) = 85 +/- 30\ \text{kev b}$

$S_{casc}(300\ \text{keV}) = 4 +/- 4\ \text{keV b}$

$S_{tot}(300\ \text{keV}) = 165 +/- 50\ \text{keV b}$

This corresponds to 1.2 times Buchman (1996) and is what has been used in KEPLER for many years.

deBoer et al 2017 (on class website)

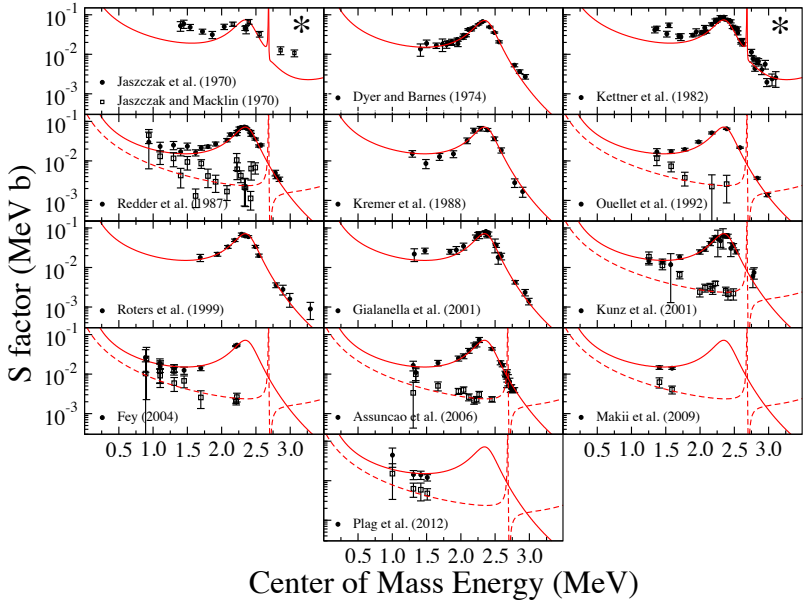

TABLE IV Extrapolations of the $^{12}C(\alpha,\gamma)^{16}O$ S-factor to $E_{c.m.} = 300$ keV categorized by either cluster model calculations are phenomenological fits. The abbreviations used below are for the generalized coordinate method (GCM) and potential model (PM) for the theoretical works and Breit-Wigner (BW), R-matrix (R), and K-matrix (K) for the phenomenological calculations. Hybrid R-matrix (HR) models have also been used in an effort to connect the phenomenological calculations more closely to more fundamental theory.

Ref.	S(300 keV) keV b $E1$	$E2$	Cascades	Total	Model
Cluster Models					
Descouvemont *et al.* (1984)	300	90			GCM
Langanke and Koonin (1985)	160-280	70	<10[c]	230-350	HR&PM
Funck *et al.* (1985)		100			PM
Redder *et al.* (1987)	140^{+120}_{-50}	80±25	7±3[c] $1.3^{+0.5d}_{-1.0}$		R&PM
Descouvemont and Baye (1987)	160	70			GCM
Ouellet *et al.* (1992)	1^{+5}_{-1}	40±7			R&PM
Descouvemont (1993)		90			GCM
Ouellet *et al.* (1996)	79±16	36±6		120±40	R,K,PM
Dufour and Descouvemont (2008)		42±2			GCM
Katsuma (2012)	≈ 3	150^{+41}_{-17}	18.0±4.5[e]	171^{+46}_{-22}	PM
Xu *et al.* (2013) (NACRE2)	80±18	61±19	$6.5^{+4.7e}_{-2.2}$	148±27	PM
Phenomenological Fits					
Burbidge *et al.* (1957)	340			340	BW
Barker (1971)	50-330			50-330	R
Koonin *et al.* (1974)	80^{+50}_{-30}			80^{+50}_{-140}	HR
Dyer and Barnes (1974)	140^{+140}_{-40}			140^{+140}_{-40}	R&HR
Weisser *et al.* (1974)	170			170	R
Humblet *et al.* (1976)	80^{+140}_{-70}			80^{+140}_{-70}	K
Kettner *et al.* (1982)	250	180	12(2)[c,d]	420^{+160}_{-120}	BW
Langanke and Koonin (1983)	150 or 340	<4% of $E1$		150 or 340	HR
Barker (1987)	150^{+140}_{-80}	30^{+50}_{-30}			R
Kremer *et al.* (1988)	0-140				R&HR
Filippone *et al.* (1989)	0-170	5-28		0-170	K
Barker and Kajino (1991)	150^{+170}_{-70} or 260^{+140}_{-160}	120^{+60}_{-70}	10[c] 1-2[d]	280^{+230}_{-140} or 390^{+200}_{-230}	R
Humblet *et al.* (1991)	43^{+20}_{-10}	7^{+24}_{-5}		50^{+30}_{-20}	K
Humblet *et al.* (1993)	45^{+5}_{-5}				K
Azuma *et al.* (1994)	79±21 or 82±26				R&K
Buchmann *et al.* (1996)	79±21	70±70	16±16[a,c,d]	165±75	R&K
Hale (1997)	20				R
Trautvetter *et al.* (1997)	79	14.5			BW
Brune *et al.* (1999)	101±17	42^{+16}_{-23}			R
Roters *et al.* (1999)	79±21				R
Angulo and Descouvemont (2000)		190-220			R
Gialanella *et al.* (2001)	82±16 or 2.4±1.0				R
Kunz *et al.* (2001)	76±20	85±30	4±4[e]	165±50	R
Tischhauser *et al.* (2002)		53^{+13}_{-18}			R
Hammer *et al.* (2005b)	77±17	81±22		162±39	R
Buchmann and Barnes (2006)			$5^{+7}_{-4.5}$[a] 7^{+13c}_{-4}		R
Matei *et al.* (2006)			25^{+16e}_{-15}		R
Matei *et al.* (2008)			7.1±1.6[c]		R
Tang *et al.* (2010)	86±22				R
Schürmann *et al.* (2011)			<1[a]		R
Schürmann *et al.* (2012)	83.4	73.4	4.4[e]	$161\pm19_{(\text{stat})}{}^{+8}_{-2(\text{syst})}$	R
Oulebsir *et al.* (2012)	100±28	50±19		175^{+63}_{-62}	R
Sayre *et al.* (2012)		62^{+9}_{-5}			R
Avila *et al.* (2015)			1.96±0.30 or 4.36±0.45[a] 0.12±0.04 or 1.44±0.12[b]		R
An *et al.* (2015)	98.0±7.0	56±4.1	8.7±1.8[e]	162.7±7.3	R
this work	86.3	45.3	7[e]	$140\pm21_{(\text{MC})}{}^{+18}_{-11(\text{model})}$	R

Current best value S_0(300 keV) = 140+-21(MC) +18-11 (model) keV barns

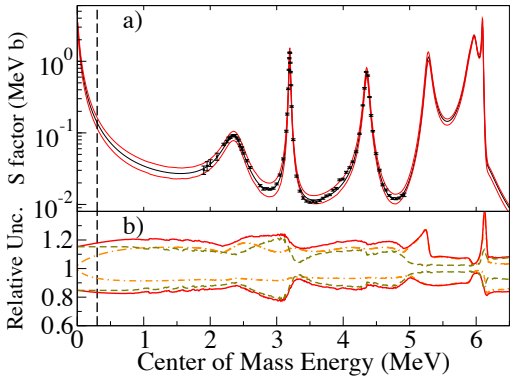

FIG. 25 (Color online) The uncertainty in the S factor as derived by combining the MC analysis (which includes the subthreshold state uncertainties) and the model uncertainties is shown in Fig. 25 a). The data from Schürmann *et al.* (2005) are shown for comparison. Fig. 25 b) shows the uncertainties relative to the best fit value for the Monte Carlo analysis (olive colored dashed line) and the uncertainties derived from the model (dot-dashed orange line). The total uncertainty, taken as the MC and model uncertainties summed in quadrature, is shown by the solid red line. The black vertical dashed line marks the region of typical astrophysical interest at $E_{\rm c.m.} = 300$ keV.

TABLE XXV The rate of the $^{12}C(\alpha,\gamma)^{16}O$ reaction. Uncertainties are calculated using a combination of Monte Carlo analysis and investigation of systematic contributions from both data and model sources and are listed separately.

T (GK)	Adopted Rate	Lower Rate	Upper Rate
0.06	6.78×10^{-26}	5.69×10^{-26}	7.90×10^{-26}
0.07	3.28×10^{-24}	2.76×10^{-24}	3.83×10^{-24}
0.08	8.00×10^{-23}	6.71×10^{-23}	9.35×10^{-23}
0.09	1.18×10^{-21}	9.91×10^{-22}	1.38×10^{-21}
0.1	1.20×10^{-20}	1.00×10^{-20}	1.40×10^{-20}
0.11	9.03×10^{-20}	7.55×10^{-20}	1.06×10^{-19}
0.12	5.38×10^{-19}	4.50×10^{-19}	6.31×10^{-19}
0.13	2.65×10^{-18}	2.21×10^{-18}	3.11×10^{-18}
0.14	1.11×10^{-17}	9.28×10^{-18}	1.30×10^{-17}
0.15	4.08×10^{-17}	3.41×10^{-17}	4.80×10^{-17}
0.16	1.34×10^{-16}	1.12×10^{-16}	1.58×10^{-16}
0.18	1.09×10^{-15}	9.11×10^{-16}	1.29×10^{-15}
0.2	6.64×10^{-15}	5.53×10^{-15}	7.83×10^{-15}
0.25	2.43×10^{-13}	2.02×10^{-13}	2.87×10^{-13}
0.3	3.73×10^{-12}	3.10×10^{-12}	4.43×10^{-12}
0.35	3.28×10^{-11}	2.72×10^{-11}	3.90×10^{-11}
0.4	1.96×10^{-10}	1.62×10^{-10}	2.33×10^{-10}
0.45	8.82×10^{-10}	7.30×10^{-10}	1.05×10^{-9}
0.5	3.22×10^{-9}	2.66×10^{-9}	3.85×10^{-9}
0.6	2.70×10^{-8}	2.23×10^{-8}	3.23×10^{-8}
0.7	1.47×10^{-7}	1.21×10^{-7}	1.76×10^{-7}
0.8	5.92×10^{-7}	4.90×10^{-7}	7.11×10^{-7}
0.9	1.92×10^{-6}	1.59×10^{-6}	2.31×10^{-6}
1	5.30×10^{-6}	4.40×10^{-6}	6.38×10^{-6}
1.25	4.10×10^{-5}	3.42×10^{-5}	4.93×10^{-5}
1.5	2.03×10^{-4}	1.70×10^{-4}	2.43×10^{-4}
1.75	7.65×10^{-4}	6.46×10^{-4}	9.14×10^{-4}
2	2.40×10^{-3}	2.04×10^{-3}	2.86×10^{-3}
2.5	1.57×10^{-2}	1.32×10^{-2}	1.88×10^{-2}
3	6.66×10^{-2}	5.51×10^{-2}	8.10×10^{-2}
3.5	2.09×10^{-1}	1.71×10^{-1}	2.55×10^{-1}
4	5.31×10^{-1}	4.37×10^{-1}	6.48×10^{-1}
5	2.38×10^{0}	2.02×10^{0}	2.84×10^{0}
6	7.93×10^{0}	6.96×10^{0}	9.22×10^{0}
7	2.11×10^{1}	1.89×10^{1}	2.41×10^{1}
8	4.64×10^{1}	4.20×10^{1}	5.26×10^{1}
9	8.75×10^{1}	7.96×10^{1}	9.86×10^{1}
10	1.46×10^{2}	1.33×10^{2}	1.64×10^{2}

Helium Burning Rate Equations

$$\frac{dY_\alpha}{dt} = -3\rho^2 Y_\alpha^3 \lambda_{3\alpha}/6 - Y_\alpha\, Y(^{12}C)\,\rho\,\lambda_{\alpha\gamma}(^{12}C)$$

$$\frac{dY(^{12}C)}{dt} = \rho^2 Y_\alpha^3 \lambda_{3\alpha}/6 - Y_\alpha\, Y(^{12}C)\,\rho\,\lambda_{\alpha\gamma}(^{12}C)$$

$$\frac{dY(^{16}O)}{dt} = Y_\alpha\, Y(^{12}C)\,\rho\lambda_{\alpha\gamma}(^{12}C)$$

For binary reactions, $\lambda \equiv N_A \langle \sigma v \rangle$

For Y_{12} small or ρ large

$$\alpha \rightarrow {}^{12}C$$

For Y_{12} large or ρ small

$$\alpha \rightarrow {}^{16}O$$

In a 15 solar mass star:

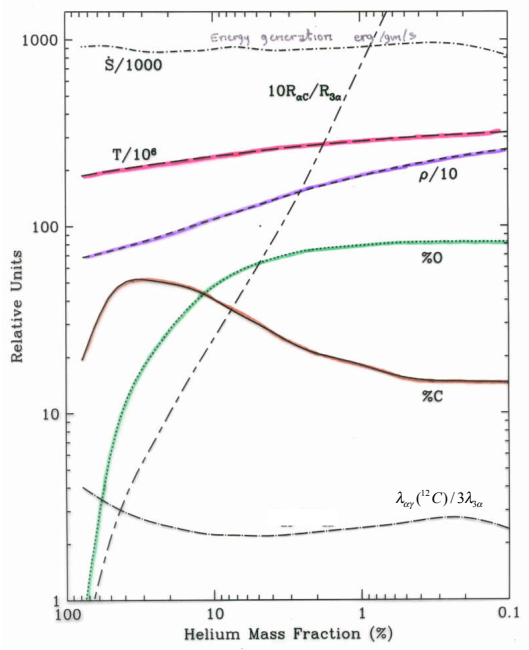

Because of the tendency of $\frac{\rho}{T^3}$ to decrease with increasing mass and the near constancy of helium burning temperatures, massive stars make a decreasing ratio of carbon to oxygen as M increases. Variation with Z reflects the different extent of convection during He burning resulting from e.g., mass loss in solar Z stars, red vs. blue supergiant

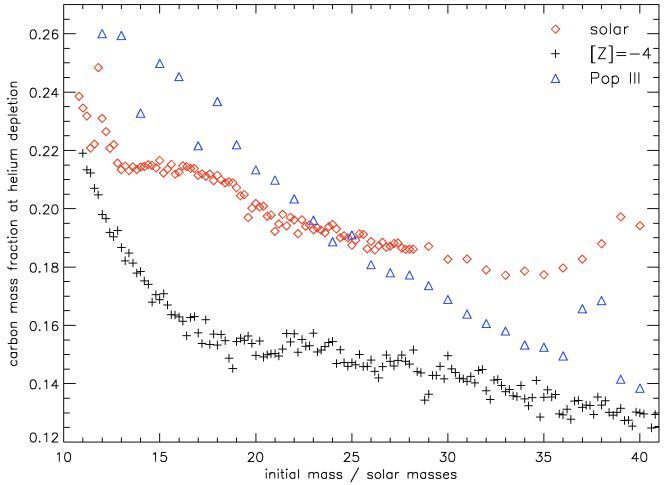

Example: Hydrogen burning

a) 100% ^{1}H $\rightarrow$ ^{4}He $\quad \delta Y(^1\mathrm{H}) = -1 \quad \mathrm{BE}(^1\mathrm{H}) = 0$

$$\delta Y(^4\mathrm{He}) = \frac{1}{4} \qquad \mathrm{BE}(^4\mathrm{He}) = 28.296\,\mathrm{MeV}$$

$$q = 9.65\times10^{17}\left(\frac{28.296}{4}\right) = 6.83\times10^{18}\ \mathrm{erg\ g^{-1}}$$

b) 70% ^{1}H; 30% ^{4}He $\rightarrow ^4$ He $\quad \delta Y(^1\mathrm{H}) = -0.7$

$$\delta Y(^4\mathrm{He}) = \frac{1}{4} - \frac{0.3}{4}$$

$$q = 9.65\times10^{17}\left(\frac{1}{4} - \frac{0.3}{4}\right)28.296 = 4.78\times10^{18}\ \mathrm{erg\ g^{-1}}$$

need to subtract off term for weak interactions and neutrino losses

Nuclear Energy Yield

When an arbitrary composition, $\{Y_i\}$, rearranges by nuclear reactions to a new composition, $\{Y_i'\}$, where $Y_i' = Y_i + \delta Y_i$, there is a change in internal energy that can be positive or negative

$$q_{nuc} = 1.602\times10^{-6}\, N_A \sum(\delta Y_i)(BE_i) \; - q_\nu \quad \mathrm{erg/gm}$$

Here 1.602 x 10^{-6} is the conversion factor from MeV (which are the units of BE) to erg and the q_ν corrects for any neutrinos that might be emitted by weak interactions or thermal processes (like pair annihilation). If there are no weak interactions and thermal neutrino losses are negligible, e.g., in helium burning, $q_\nu = 0$.

BE(^{12}C) = 92.162 MeV
BE(^{16}O) = 127.619
BE(α) = 28.296 MeV
} values for helium burning

A related quantity, the energy generation rate is given by

$$\dot{\varepsilon}_{nuc} = 9.65\times10^{17} \sum \frac{dY_i}{dt}(BE_i) - q_{\nu,weak} - q_{\nu,thermal} \ \mathrm{erg\ g^{-1}\ sec^{-1}}$$

Both these expressions are only good for strong interactions. In a weak interaction one has to worry about n and p mass differences, electron masses created and destroyed, as well as the mean neutrino energy loss.

A correct expression uses the atomic mass excesses. To within a constant

$$\dot{\varepsilon}_{nuc} = -\sum_i \frac{dY_i}{dt} M_i({}^A Z)\,[-\text{neutrino losses}] \qquad \text{where}$$

$$M_i = \mathrm{A}_i(931.49) + \Delta_i \ \text{MeV} \qquad \text{and}$$

$$BE = Z\Delta_H + N\Delta_n - \Delta({}^A Z) \quad \text{and} \quad \sum_i \frac{dY_i}{dt} A_i = \sum_i \frac{dX_i}{dt} = 0 \quad \text{so that}$$

$$\dot{\varepsilon}_{nuc} = \sum_i \frac{dY_i}{dt} BE_i - \sum_i \frac{dY_i}{dt}\left(Z_i\Delta_H + N_i\Delta_n\right) \quad [-\text{neutrino losses}]$$

In the absence of weak interactions the second and third term may be dropped.(this includes the energy that the positrons deposit when they annihilate in positron emission).